Send Orders for Reprints to reprints@benthamscience.ae

Current Alzheimer Research, **2015,** *12,* **481-492**

1950 MHz Electromagnetic Fields Ameliorate Aβ Pathology in Alzheimer's Disease Mice

Ye Ji Jeong[1,#], Ga-Young Kang[2,#], Jong Hwa Kwon[3], Hyung-Do Choi[3], Jeong-Ki Pack[4], Nam Kim[5], Yun-Sil Lee[2,*] and Hae-June Lee[1,*]

Yun-Sil Lee

[1]Division of Radiation Effects, Korea Institute of Radiological & Medical Sciences, Seoul, 139-706, Korea; [2]Graduate School of Pharmaceutical Sciences, Ewha Womans University, Seoul, 120-750, Korea; [3]Department of EMF Research Team, Radio and Broadcasting Technology Laboratory, ETRI, Daejon, 305-700, Korea; [4]Department of Radio Sciences and Engineering, College of Engineering, Chungnam National University, Daejon, 305-764, Korea; [5]School of Electrical and Computer Engineering, Chungbuk National University, Cheongju,Chungbuk,362-763, Korea

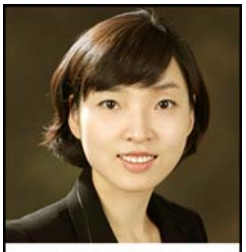

Hae-June Lee

Abstract: The involvement of radiofrequency electromagnetic fields (RF-EMF) in the neurodegenerative disease, especially Alzheimer's disease (AD), has received wide consideration, however, outcomes from several researches have not shown consistency. In this study, we determined whether RF-EMF influenced AD pathology *in vivo* using Tg-5xFAD mice as a model of AD-like amyloid β (Aβ) pathology. The transgenic (Tg)-5xFAD and wild type (WT) mice were chronically exposed to RF-EMF for 8 months (1950 MHz, SAR 5W/kg, 2 hrs/day, 5 days/week). Notably, chronic RF-EMF exposure significantly reduced not only Aβ plaques, APP, and APP carboxyl-terminal fragments (CTFs) in whole brain including hippocampus and entorhinal cortex but also the ratio of Aβ42 and Aβ40 peptide in the hippocampus of Tg-5xFAD mice. We also found that parenchymal expression of β-amyloid precursor protein cleaving enzyme 1(BACE1) and neuroinflammation were inhibited by RF-EMF exposure in Tg-5xFAD. In addition, RF-EMF was shown to rescue memory impairment in Tg-5xFAD. Moreover, gene profiling from microarray data using hippocampus of WT and Tg-5xFAD following RF-EMF exposure revealed that 5 genes (Tshz2, Gm12695, St3gal1, Isx and Tll1), which are involved in Aβ, are significantly altered inTg-5xFAD mice, exhibiting different responses to RF-EMF in WT or Tg-5xFAD mice; RF-EMF exposure in WT mice showed similar patterns to control Tg-5xFAD mice, however, RF-EMF exposure in Tg-5xFAD mice showed opposite expression patterns. These findings indicate that chronic RF-EMF exposure directly affects Aβ pathology in AD but not in normal brain. Therefore, RF-EMF has preventive effects against AD-like pathology in advanced AD mice with a high expression of Aβ, which suggests that RF-EMF can have a beneficial influence on AD.

Keywords: Alzheimer's disease mice, β-amyloid, BACE1, microarray, radiofrequency electromagnetic field.

INTRODUCTION

The increased use of mobile phones has generated public concerns about the impact of radiofrequency electromagnetic fields (RF-EMF) on health. Because EMF emitted by a mobile phone is usually absorbed by the head and brain, RF-EMF may affect brain functions. Therefore, initial concerns were that RF-EMF exposure may induce health problems such as brain cancer [1, 2]. However, the recent 13-nation INTERPHONE study [3, 4] and numerous epidemiologic studies [5-7] conclude that no consistent evidence has indicated that long-term RF-EMF exposure can cause brain tumors.

*Address correspondence to these authors at the Graduate School of Pharmaceutical Sciences, EwhaWomans University, Seoul 120-750, Korea;
Tel: 82-2-3277-3022; Fax: 82-2-3277-2851; E-mail: yslee0425@ewha.ac.kr
and Division of Radiation Effects, Korea Institute of Radiological & Medical Sciences, Seoul, 139-706, Korea; Tel: 82-2-970-1638;
Fax: 82-2-970-1985; E-mail: hjlee@kirams.re.kr

#These authors contributed equally to this work

Currently, there is a debate about the effects of RF-EMF on memory and learning behavior and studies have reported harmful effects [8-11], no significant influences [12,13] and even beneficial effects [14-17]. Interestingly, the beneficial effects of RF-EMF exposure were usually observed in the Alzheimer's disease (AD) pathology transgenic model [14-18], which indicates that RF-EMF may affect AD pathology. In addition, most papers that reported no significant beneficial or impaired effects on cognitive performance were conducted with single acute exposure. Therefore, it is necessary to investigate whether chronic exposure to RF-EMF, using an AD-like pathology animal model, affects brain functions.

AD is a progressive neurodegenerative disorder that is characterized by cognitive and memory deterioration. One of the pathological hallmarks of AD is the abnormal accumulation of amyloid-beta protein (Aβ) in the brain. The Aβ mechanism of neurotoxicity has been hypothesized, but has not yet been proven. However, an AD animal model that

1875-5828/15 $58.00+.00

exhibits Aβ pathology is very useful for studying AD-like pathology including memory and learning deficits. Additionally, changes in production, processing, and/or clearance of brain Aβ levels are believed to be key events in the pathophysiology of both sporadic and early onset AD.

In this study, we used the 5xFAD mouse model, with this mouse overexpressing both APP with K670N/M671L (Swedish mutation), 1716V (Florida mutation), and V7171 (London mutation), and PS1 with the M146L and L286 mutations. The 5xFAD mice exhibited a very aggressive Aβ deposition that develops intraneuronal Aβ at 1.5 months, plaques at 2 months, memory deficits at 4 months and neuron death at 9 months of age [19]. The mice were exposed to 1950 MHz RF-EMF with SAR 5W/kg, which is a relatively high SAR dose and non-thermal conditions for 8 months. After 8 months the mice were examined for relatively chronic exposure conditions and AD-like pathology including Aβ deposition and neuroinflammation.

MATERIALS AND METHODS

Animals

We used female transgenic 5xFAD mice (a gift from Dr. InheeMook-Jung, Seoul National University) that contained five mutant human genes associated with Alzheimer's disease, three amyloid precursor protein (APP) genes (APPsw, APPfl, APPlon) and two presenilin1 (PS1, PSEN1) genes (PSEN1 M146L, PSEN1 L286V). The generation of the 5xFAD mice was described previously [20]. We used female WT and Tg-5xFAD mice and assigned the mice to the following groups; WT-control (n=7), WT-RF exposure (n=7), Tg-5xFAD control (n=10) and Tg-5xFAD RF exposure (n=11). RF-EMFexposure was started at an age of 1.5 months with animals are adolescent with immature brain since intraneuronal Aβ aggregation developed genetically in Tg-5xFAD mice from this point of time. All mouse procedures in this study were approved by the Institutional Animal Care and Use Committee of the Korea Institute of Radiological and Medical Sciences (IACUC permit number: KIRAMS2013-67).

RF Exposure System

Whole-body exposure to RF-EMF of 1,950 MHz was performed in a reverberation chamber designed to allow *in vivo* experiments. Detailed descriptions of the system, the uniformity of the field dose, and the SAR have been given previously [21]. Briefly, generation of a 1,950 MHz RF-EMF signal was achieved using a microprocessor unit (MPU) chip on which WCDMA-formatted coding controlled a central processing unit (CPU), and the signal was subsequently amplified using an additional high-power amplifier (PCS60WHPA_CW; Kortcom Co., Anyang, Gyeonggi-do, Korea) after passage through a separate digital attenuator. An 11-bit digital PIN diode attenuator (Model 349; General Microwave, Farmingdale, NY) was used to control the output power level (maximum: 60 W). The transmitting antennae used were commercial products (patch type, KCAN1900PA; Korea Telecommunication Components, Kyunggi-do, South Korea). A computer was used to control exposure level and time. The external dimensions of the reverberation chamber were 2,295 mm x 2,293 mm x 1,470 mm; the walls were made of stainless steel with a thickness of 2.3 mm. To measure field uniformity, five cages were placed in the test area and the field strength was measured for 1 min at each of 24 points. The distribution of the electric field inside the chamber was determined using a three-axis isotropic probe (HI-6005; ETS-Lindgren, Cedar Park, TX). Any difference in field distribution was much less than 3 dB. The SAR distribution for each caged mouse was calculated using a mouse phantom (Chungnam National University, Daejon, Korea); simulation featured 40 tissues and a voxel size of 1 mm. The power output was controlled at 52 W to achieve an average whole-body SAR of 5 W/kg. A reverberation chamber was placed in the animal facility, and the ventilation, temperature and humidity were controlled. The animals were exposed to 1,950 MHz RF-EMF according to the following schedule: SAR 5 W/kg, 2 h/day, 5 days/week, for 8 months. All animals were placed inside chambers exposed or not to RF-EMF signals. During RF exposure, the air temperature in the test area inside was maintained at 20 ± 3°C. Rectal temperatures were measured before RF-EMF exposure and immediately thereafter. Body temperature did not increase by over 0.5°C (the changes ranged from -1.9 to +0.5°C), and the temperature was thus maintained within the normal range.

Tissue Preparation

Mice were sacrificed to harvest the brain tissue after behavioral tests at 8 months after RF exposure. For histological analysis, the left hemispheres of 3 mice per group were fixed in 4% paraformaldehyde solution. The right hemispheres were (3 mice) fixed in RNA later® (Qiagen, USA) overnight at 4°C and the hippocampus was dissected from the brain and stored at -80°C for the microarray and PCR analysis. The hippocampus and entorhinal cortex, according to the atlas of Paxinos and Franklin [22], of 3 mice from each group were dissected for Western blotting analysis. The other brains were assigned to histology, PCR and Western blotting assay in the same ratios.

ELISA

Enzyme-linked immunospecific assay was performed to measure β-amyloid 40 and 42 proteins in the cerebral tissue (Covance, NJ, USA) were quantified by commercial ELISA kits following the manufacturer's protocol. Briefly, samples were diluted in sample diluent to detect Aβ40 and Aβ42 levels within an optimal working range of each standard at known concentrations (0-500 pg/ml). Following incubation with antibody solutions and the concentration in the sample was determined by colometric assay with the absorbance at 620 nm (A_{620}). A_{620} values were converted to pg Aβ40 or pg Aβ42/mg tissue by correcting dilution factors and dividing by the weight of tissue.

Immunohistochemistry and Immunofluorescence

Brain samples were fixed in 4% paraformaldehyde, paraffin-embedded, and sectioned with 5 μm. Immunostaining of sections was conducted with Vectastain Elite ABC kit (Vector Laboratories Inc, USA) following the manufacturer's protocol. For antigen retrieval, the sections were placed in citrate buffer (pH 6.0) and heated in boiling water

for 30 minutes. For immunoperoxidase labeling, endogenous peroxidase was blocked by 0.3% H_2O_2 in absolute methanol for 15 minutes at room temperature.

For immunohistochemistry, sections were blocked with normal horse serum (Vector Laboratories Inc), then incubated overnight at 4°C with anti-human Aβ antibody (1:100, #2450, Cell Signaling, MA) or anti-mouse BACE1 (1:100, 61-3E7, Santa Cruz, TX), next incubated with biotinylated goat anti-human or mouse IgG (Vector Laboratories Inc) for 3 min at RT. Immunoreaction with an avidin-biotin peroxidase complex (prepared according to the manufacturer's instructions; Vector Laboratories Inc) next proceeded for 30 min at RT. The peroxidase reaction was developed using the DAB kit (Vector Laboratories Inc). As a control, the primary antibody was omitted for a few test sections in each experiment. Sections were counterstained with Harris' hematoxylin prior to mounting.

For immunofluorescence, sections were blocked with normal horse serum (Vector Laboratories Inc), then incubated overnight at 4°C with anti-goat GFAP antibody (1:1000, ab53554, Abcam, UK), washed, and incubated with the appropriate secondary antibodies (Alexa 488-labeled anti-goat IgG) for 2 hrs at RT. After washing, the sections were counterstained with DAPI and mounted. Image J was used to quantify the amount of Aβ in the brain section.

Western Blotting

Brain tissues were minced and placed in tissue lysate buffer (Pro-prep™, Intron Inc., Korea). Protein concentration was determined by protein assay (Bio-Rad, CA, USA). Western blot analysis was performed using the following antibodies: anti-mouse BACE1, anti-goat GFAP, anti-mouse Iba1 (ab15690, Abcam, UK), and β-actin (Sigma, MO, USA). And anti-rabbit APP-CTF (A8717, Sigma) was used to detect full-length APP (FL-APP) and CTFs of APP. Quantification of Western blotting was performed using Image J, comparing individual band with band intensities on the same gel. Three brain samples from hippocampus and cortex per each group were used for Western blotting.

Reverse Transcriptase PCR (RT-PCR)

After extracting of total RNA using TRIzol® Reagent, RNA was reverse-transcribed with the ampiRiver Platinum cDNA Synthesis Master Mix Kit (GenDEPOT, Barker, TX) according to the manufacture's instruction. 5X reaction buffer (with dNTPs), ExAct™ Plus *Taq* polymerase, and sense and antisense primers were then added and the RT-PCR experiments were performed on the XP Thermal Cycler (BIOER Technology, Japan). The primers used for RT-PCR are shown in (Table **1**). The relative expressions of genes were normalized to those of the housekeeping gene encoding β-actin. Three brain samples from hippocampus and cortex were analyzed for RT-PCR.

Behavioral Test

Behavioral dysfunction in WT and Tg-5xFAD mice that received chronic RF-EMF exposure were measured using the open field test, Y-maze test, and a passive avoidance test. The order of testing was open field, Y-maze, and passive avoidance. During testing, the experimenter was blinded to the treatment given to the mice.

Table 1. Primer sequences for RT-PCR analysis.

Gene Symbol	Primer Sequence	Size
NEP	Sense: TGGACTCCCCTGGAGATCAG Antisense: ACCAGCCTCCACAAGCATAC	205
IDE	Sense: GACAGAGGAGGCGTTCCAAA Antisense: TTCACGAGGGGAAACAGTGG	396
β-actin	Sense: TGCTTCTAGGCGGACTGTTACTGA Antisense: TCGCCTTCACCGTTCCAGTTTT	223

The open field test was used to assay the general activity of the mice. Mice were placed in the central area of acrylic chamber (60 × 60 × 50 cm) and video tracking was started. Mice were allowed to move without restrictions for 30 minutes in the open field apparatus. The footpath of all the animals was recorded by the automated video-tracking system (Viewer3, BIOSERVE GmbH, Germany). The tracking system was used to quantify the total track lengths traveled and the time was tracked in the central region of the apparatus.

The Y-maze test was used to measure the working memory and reference memory, which were assessed by recording spontaneous alternation behavior. The activity was recorded for 8 minutes and analyzed by a computer program. Alternation was defined as successive entries into the three different arms on overlapping triplet sets. Percentage alternation was calculated as the ratio of actual to possible alternation (defined as the total number of arm entries minus two), multiplied by 100 as shown by: % Alternation = {(No. of alternations) / (Total arm entries – 2)} X 100.

The passive avoidance test was used to assess the response to aversive stimulus and long-term memory. The apparatus consisted of two divided rooms and a grilled floor to conduct an electric stimulation. The steel board separated the two rooms and could automatically be moved up and down. In the adaptation session, mice traveled freely between both the rooms for 5 minutes. The next day, the rooms were divided and each mouse was placed in one room. The room was kept dark for 30 seconds to allow the mouse to adjust, and then the light was turned on simultaneously moving the steel panel. As the mouse traveled across to the other room to avoid the bright light, the movement shut down the steel panel and an electrical shock impulse (1 mA, 5s) was transmitted on the grill. After 24 hrs, the mice were subjected to the same trial without electrical shock and the latency time to cross over to the other room was recorded.

Microarray Analysis

To synthesize target cRNA probes and hybridization, microarrays were performed using a Low RNA Input Linear Amplification kit (Aligent Technology, USA), following the manufacturer's protocols, at ebiogen (Seoul, Korea). The gene expression levels were calculated by dividing the average of the normalized signal channel intensity by the average of the normalized control channel intensity.

Quantitative Real-Time PCR (qRT-PCR)

Total RNA was isolated using TRIzol® Reagent (Molecular Research Center, Cincinnati, OH, USA) and reverse transcribed into cDNA using a ReverTra Ace®qPCR RT Kit (TOYOBO, Osaka, Japan), as described by the manufacturer. The qRT-PCR was performed using gene-specific primers with Power SYBR® Green PCR Master Mix (Invitrogen, Carlsbad, CA, USA). The full list of primers used can be found in Table **2**. The qRT-PCR experiments were performed on the 7300 Real Time PCR System (Applied Biosystems, Foster City, CA, USA).

Table 2. Primer sequences for qRT-PCR analysis.

Gene Symbol	Primer sequence
Tshz2	Sense: CCACAGAAAGACGAGCGAGA Antisense: TCAGGACCTTTTGGGCATCC
Isx	Sense: GCAGGAGAAGAGTGGGAACC Antisense: ACAGGACCAGACACGTCCAT
Tll1	Sense: AGGCTTTTAAGGTCTGGCGG Antisense: CTGGGAAGCTCCTCGGAAAG
St3gal1	Sense: GTTTGAGCTGGCTGGGTTTG Antisense: AAGCGCTGGTCGAACCAATA
Gm12695	Sense: TGACGTCAGCACCAGAAGAC Antisense: AAGGCCTGGTTGATTCTCCG

Statistical Analysis

Data were analyzed using two-tailed *t*-test for comparison between groups and ANOVA (analysis of variance) and Bonferroni post-hoc test for multiple comparisons. All data are presented as mean ± standard error of the mean (SEM). Significance was taken when the *p*-value was less than 0.05.

RESULT

Chronic RF-EMF Exposure Reduces Aβ Deposition

We used 5xFAD transgenic mouse models (Tg-5xFAD) genetically designed to show Aβ overproduction and memory deficits, to investigate the effect of RF-EMF on an AD brain. Animals were sacrificed at 8 months after RF-EMF exposure (9.5 months old). ELISA assay indicated that RF-EMF exposed Tg-5xFAD mice had a significant reduction in the amount of cerebral Aβ, with a significant reduction of Aβ40 (8.6-fold in the hippocampus and 7.2-fold in the cortex) and Aβ42 (11.2-fold in the hippocampus and 2.6-fold in the cortex), when compared to the control Tg-5xFAD mice (Table **3**). Furthermore, RF-EMF exposure reduced the ratio of Aβ42 and Aβ40 by 70% in the hippocampus compared to control Tg groups (Fig. **1A**). The relative levels of the Aβ42 and Aβ40 peptide species, and the specific Aβ42 and Aβ40 ratio were suggested to have a pivotal role in AD pathogenesis. Immunohistochemistry analysis for Aβ on brain sections from WT and Tg-5xFAD mice following RF exposure focused on CA1 of the hippocampus and entorhinal cortex, which is known as a main lesion in AD pathology. This analysis revealed that Tg-5xFAD AD mice showed severe Aβ deposition throughout the brain including the hippocampus and entorhinal cortex while that of WT mice showed no Aβ deposition in the brain (Fig. **1B**). Surprisingly, there was a remarkable decrease in both the numbers and the size of Aβ plaques in RF-exposed Tg-5xFAD mice. Area quantification of Aβ plaques in the brain section indicated that RF-EMF reduced 30%, 15% and 10% of Aβ deposition in the hippocampus, entorhinal cortex region, and whole brain area, respectively, compared to the control Tg-5xFAD AD mice (Fig. **1C**). These results were consistent with the Aβ content results from the ELISA analysis.

Changes in the Levels of FL-APP, CTFs, and A β Degrading Enzymes in the Brain After RF-EMF Exposure

To determine whether APP processing and Aβ protein degradation were affected by RF-EMF exposure, Western blotting and RT-PCR were done on brain tissue. As illustrated in Fig. (**2A**), no differences were found in the levels of FL-APP and CTFs of APP in wild type mice. However, FL-APP levels increased both in the hippocampus and cortex of 5xFAD mice. Concomitantly, an elevation of CTFs of APP was also found in the 5xFAD mice brain. After chronic RF-EMF exposure, the levels of APP and CTFs of APP were

Table 3. Aβ ELISA of wide type and Tg-5xFAD mice.

		Wide Type		Tg-5xFAD	
		Con	RF	Con	RF
	No. of Samples	3	4	6	6
Hippocampus	Aβ42	65 ± 25	52 ± 17	1982 ± 85	177 ± 28*
	Aβ40	72 ± 55	98 ± 40	1424 ± 221	548 ± 309*
Cortex	Aβ42	123 ± 39	70 ± 34	2031 ± 429	146 ± 86*
	Aβ40	65 ± 6	82 ± 32	1713 ± 138	237 ± 162*

The unit is pg/mg.
Data presented are the mean ± SEM.
*p<0.01; RF treated Tg-5xFAD compared to control Tg-5xFAD.

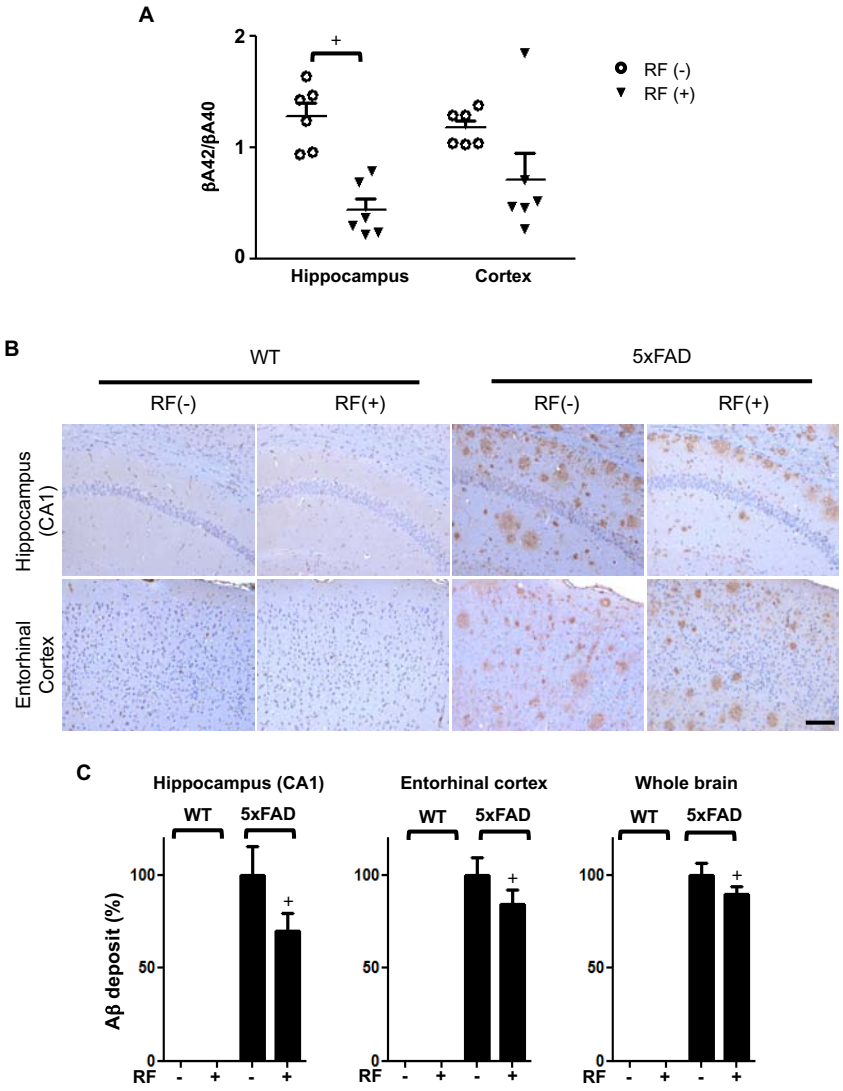

Fig. (1). Chronic RF-EMF exposure reduces Aβ deposition in Tg-5xFAD mice. A. Aβ in Tg-5xFAD and WT mice at the age of 9.5 months following RF-EMF exposure for 8 months. The Aβ42 and Aβ40 in the brain lysate of Tg-5xFAD mice were measured by color metric ELISA assay. The graph shows a ratio of Aβ42 peptide and Aβ40 in lysates of the hippocampus and entorhinal cortex. **B.** Representative images of Aβ deposition in the CA1 region of the hippocampus and entorhinal cortex of Tg-5xFAD and WT mice. Brown spots indicate Aβ plaques. Scale bar: 100μm. **C.** Quantification of Aβ deposition in hippocampus, entorhinal cortex and whole brain area. Data indicate arbitrary value compared to control Tg-5xFAD mice. Values are presented as the mean ± SEM (n=6). Statistical differences were established by two-tailed *t*-test analysis for comparison between 5xFAD-RF(-) and Tg-5xFAD-RF (+) for *p*-value less than 0.05.

decreased in the hippocampus and cortex of the 5xFAD mice brain. However, levels of the Aβ-degrading enzymes, including neprilysin (NEP) and insulin-degrading enzyme (IDE), were not affected by RF-EMF exposure both in WT and 5xFAD mice (Fig. **2B**).

RF-EMF Exposure Modulates BACE1 Expression in the Brain

To determine whether BACE1 was affected by RF-EMF exposure, immunostaining for BACE1 was done on brain sections and elevated BACE1 expression patterns were found in both the hippocampus and entorihnal cortex region of Tg-5xFAD mice, when compared to that of WT mice (Fig. **3A**). However, RF-EMF-exposed Tg-5xFAD mice showed a significant reduction in BACE1 expression on brain section when compared to control Tg-5xFAD mice. We confirmed BACE1 expression by Western blot, using brain homogenates and obtained similar results (Fig. **3B**). For WT mice, a slight induction of BACE1 by RF-EMF exposure was detected, which was opposite to the Tg-5xFAD mice results.

RF-EMF Exposure Decreases Neuroinflammatory Cells

Tg-5xFAD mice had higher expression of GFAP, a marker of activated astrocytes, than WT mice. Tg-5xFAD mice showed extensive GFAP positive signaling, when compared to WT mice (Fig. **4A**). The elevated GFAP was also confirmed by Western blotting brain homogenates from different parts of the brain, hippocampus and entorhinal cortex (Fig. **4B**). However, the hippocampus and entorhinal cortex

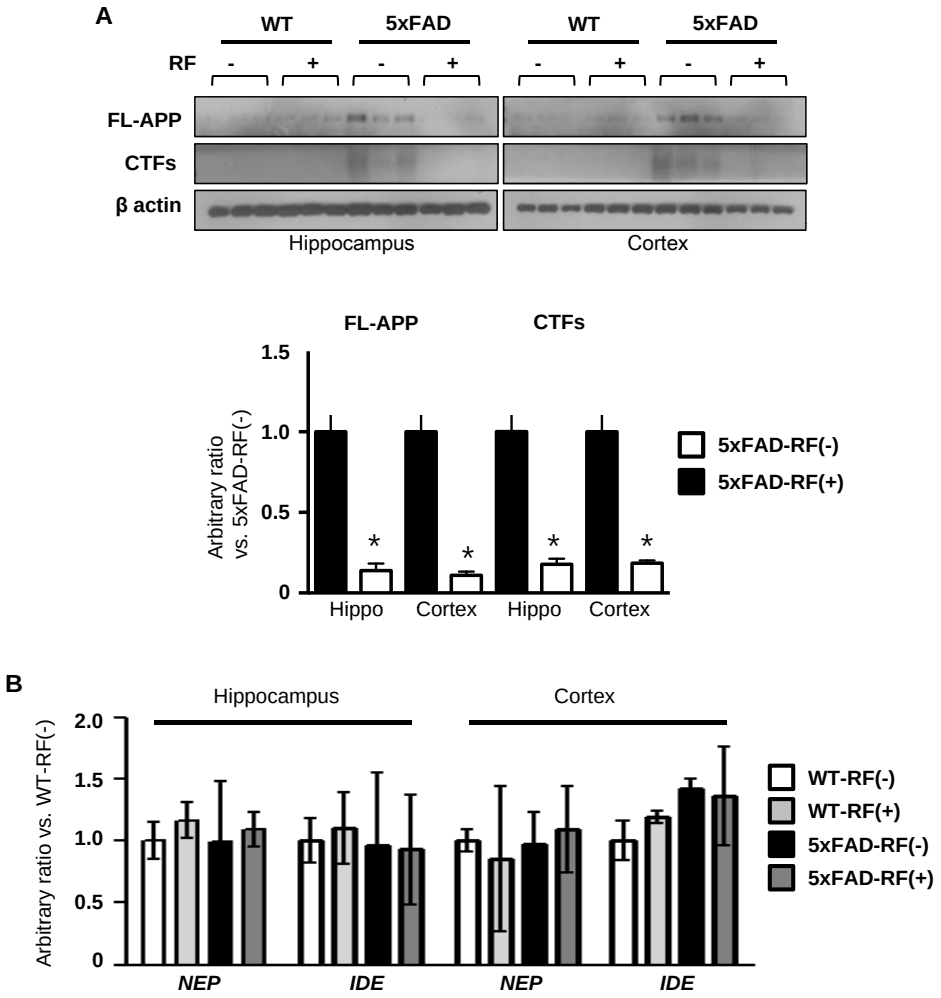

Fig. (2). Effects of chronic RF-EMF in the expressions of APP, CTFs and Aβ-degrading enzymes in WT and Tg-5xFAD mice brain. A. Western blotting of FL-APP and CTFs of APP in the hippocampus and cortex extract in Tg-5xFAD and WT mice following RF-EMF exposure. The graph showed quantification of expression of APP and CTFs using band intensity of Tg-5xFAD mice. Values are presented as the mean ± SEM (n=3) and analyzed by two-tailed *t*-test (* $p < 0.05$ Tg-5xFAD (RF-) *vs.* Tg-5xFAD-RF (+)). **B.** A RT-PCR for Aβ-degrading enzymes genes, including *NEP* and *IDE*, performed using hippocampus and cortex tissues from WT and Tg-5xFAD mice with or without RF-EMF exposure. Values are presented as the mean ± SEM (n=3) and analyzed by ANOVA (analysis of variance) and Bonferroni post-hoc test.

of RF-EMF-exposed brain section showed dramatically reduced GFAP expression. In the case of WT mice, RF exposure showed no effect or slightly elevated effect on GFAP expression.

Immunoblotting data for Iba1, a marker for activated microglia, showed similar effects with GFAP expression; lower Iba1 expression in RF-EMF-exposed Tg-5xFAD mice than in control Tg-5xFAD mice. Iba1 expression in WT mice was not altered in the hippocampus but was slightly decreased in the entorhinal cortex with RF-EMF exposure (Fig. **4B**).

RF-EMF Exposure Ameliorates Memory Impairment

Next, we explored whether RF-EMF exposure affected the memory functions of AD mice. Tg-5xFAD animals aged 9.5 months exhibited slight motor impairment, although WT and Tg-5xFAD animals were similar in terms of exploratory locomotor activity (measured by total distance traveled). RF-EMF exposure slightly increased the total distance travelled, although this was not statistically significant. Time spent in the center, reflecting anxiety-related behavior, was higher in Tg-5xFAD mice than in the wild-type animals, and exposure to RF-EMF reduced this time in Tg-5xFAD animals but not in the wild-type mice (Fig. **5A**).

Passive avoidance testing was performed to evaluate learning and memory. These functions were not affected upon exposure of wild-type mice to RF-EMF, but Tg-5xFAD mice exhibited significant memory impairment. RF-EMF exposure significantly extended the step-through latency of Tg-5xFAD mice (Fig. **5B**). We also evaluated the effect of RF-EMF on spatial memory using the Y-maze test. Fig. (**5C**) shows that RF-EMF exposure significantly compensated the impaired spatial memory of Tg-5xFAD mice, but wild-type animals did not derive any benefit from RF-EMF exposure.

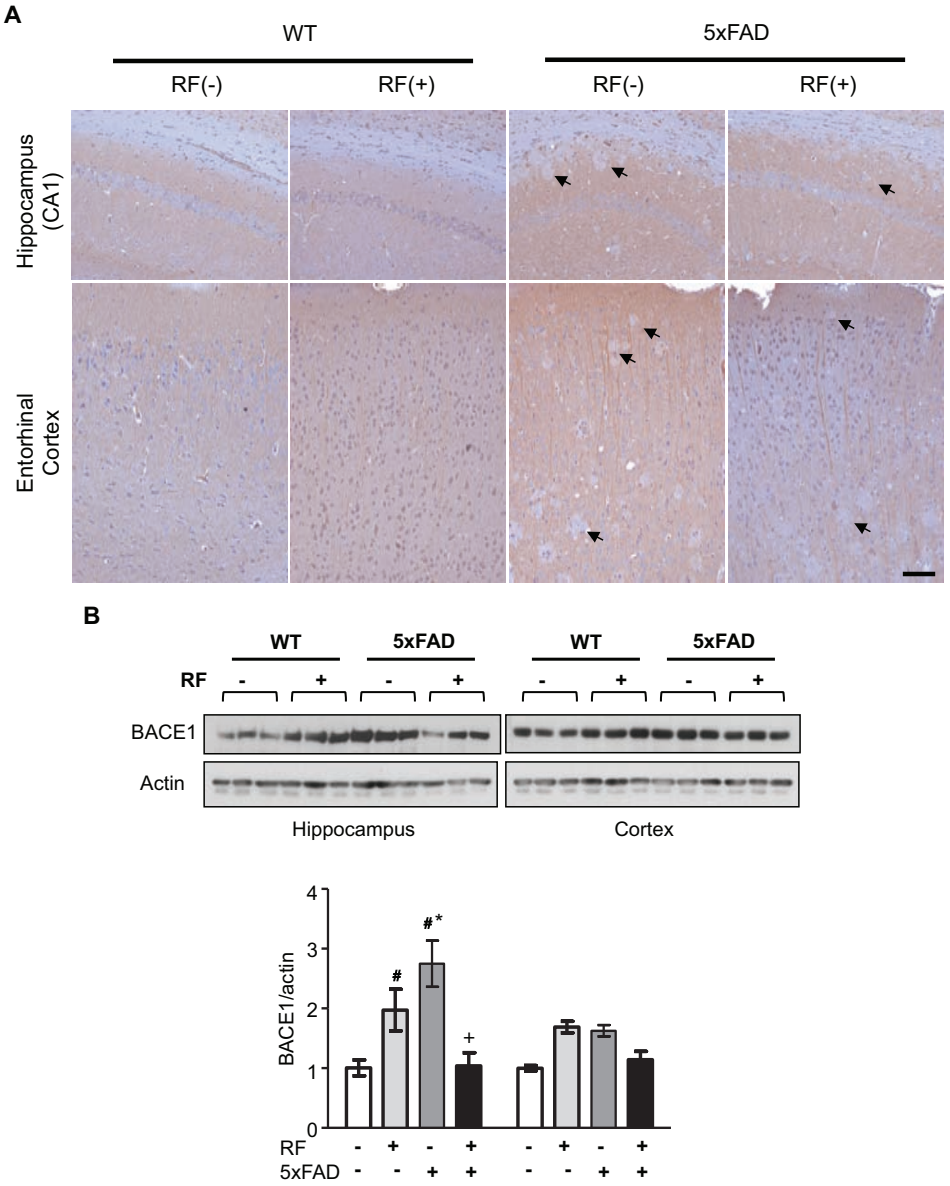

Fig. (3). RF-EMF modulates BACE1 expression. A. Immunohistochemistry analysis of BACE1 expression in brain sections following chronic RF-EMF exposed Tg-5xFAD and WT mice. Arrow indicates BACE negative Aβ plaques. Scale bar: 100μm. **B.** Western blotting of BACE1 in the hippocampus and cortex extract in Tg-5xFAD and WT mice following RF-EMF exposure. Values are presented as the mean ± SEM and analyzed by ANOVA (analysis of variance) and Bonferroni post-hoc test (# $p < 0.05$ *vs.* WT-RF(-), * $p < 0.05$ *vs.* WT-RF (+), + $p < 0.05$ *vs.* Tg-5xFAD-RF (-)).

RF-EMF Exposure Alters Aβ-Related Gene Expression

To further elucidate the effect of RF-EMF on the brain, we performed a microarray to comprehensively profile gene expression patterns in the hippocampus of WT and Tg-5xFAD mice following RF-EMF exposure. We selected genes categorized in behavior and behavior mechanism, disciplines and activities, and mental disorder (Supplementary Table **1**) and examined gene expression patterns using the microarray system. Genes were differentially expressed (more than 2-fold up or down) in Tg-5xFAD mice when compared to WT mice (Fig. **6A** and Table **4**). Genes that could be responsible for AD development were selected for analysis. After the microarray data was confirmed by qRT-PCR using hippocampal tissues (Fig. **6B** and Table **4**), five genes were collected. Heat map analysis of these genes revealed that RF-EMF exposure in WT mice showed similar patterns with gene expression in Tg-5xFAD mice without RF-EMF exposure when WT mice were used as a control. However, for RF-EMF exposed Tg-5xFAD mice, the heat map patterns were completely different from RF-EMF exposed WT mice. The Tshz2, Ggm1265 and St3gal1 genes were altered in Tg-5xFAD mice when compared to WT mice; analysis of RF-EMF exposure indicated similar patterns which suggest that these genes could be related to AD development. Other genes such as Isx and Tll1 had similar expression patterns between RF-EMF-exposed WT mice and control Tg-5xFAD mice when WT mice were used as a control. However, these expression patterns were reversed in

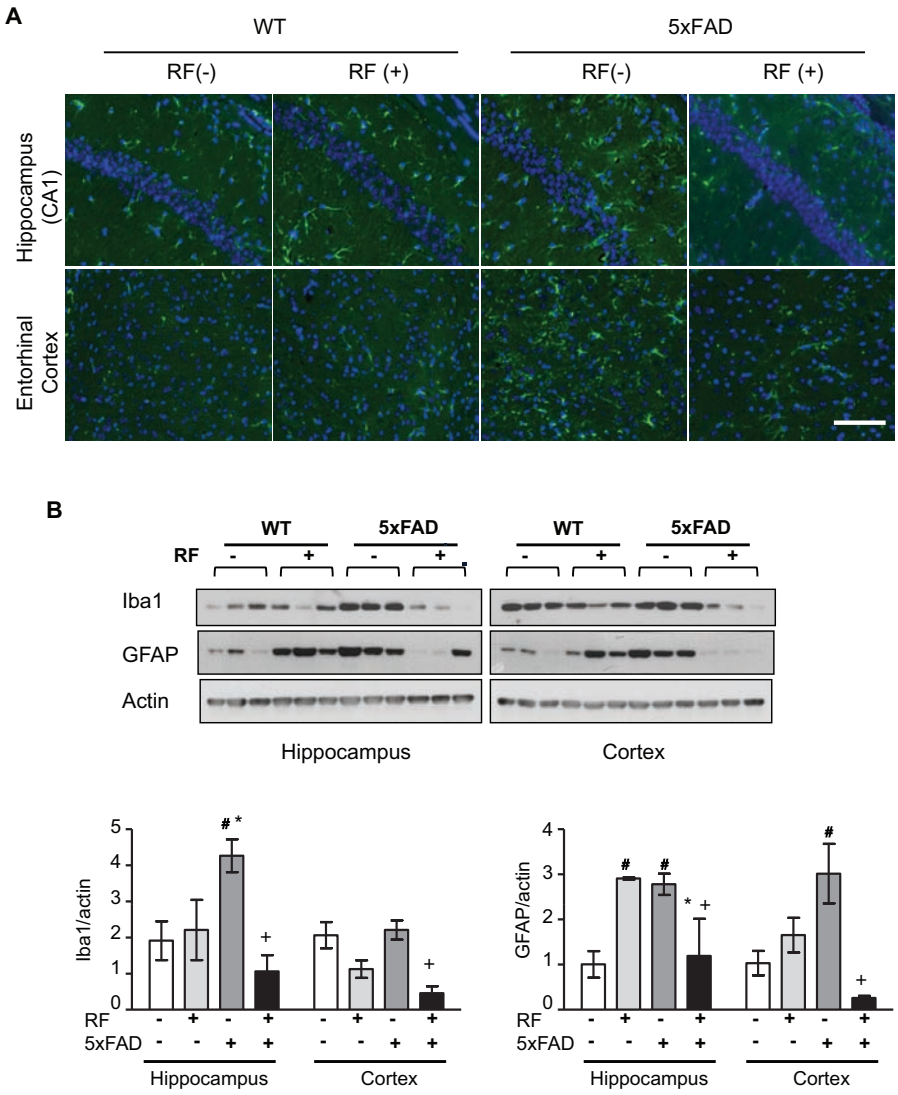

Fig. (4). Decreased reactive astrocytes and active microglia in Tg-5xFAD mice by RF-EMF exposure. A. Immunofluorescence staining of GFAP (green) and DAPI (blue) in the hippocampus (CA1 region) and entorhinal cortex of brain sections from WT and Tg-5xFAD mice following RF-EMF exposure. Scale bar: 100 μm. **B.** Western blotting of Iba1 and GFAP in the hippocampus and cortex lysate. Actin was used as a loading control. Values are presented as the mean ± SEM and analyzed by ANOVA (analysis of variance) and Bonferroni post-hoc test (# $p < 0.05$ *vs.* WT-RF(-), * $p < 0.05$ *vs.* WT-RF (+), + $p < 0.05$ *vs.* Tg-5xFAD-RF (-)).

Tg-5xFAD mice after RF-EMF exposure, suggesting that there are RF-EMF specific genes that provide beneficial brain functions in AD mice.

DISCUSSION

This study aimed to investigate the effects of RF-EMF on Alzheimer's disease based on Aβ pathology. We used a 5xFAD transgenic mouse model which has AD-like pathology and accumulates large amounts of Aβ in the brain parenchyma. Although data about the role of Aβ in AD remain controversial, Aβ plaque-based transgenic models are very useful for studying AD-like pathologies, such as memory impairment [23]. We exposed Tg-5xFAD and WT mice to RF-EMF for 8 months to evaluate the effect of RF-EMF on memory impairment and Aβ pathology. To exclude the thermal effects of RF-EMF, we used an *in vivo* RF-EMF exposure chamber that allows free movement during RF-EMF exposure and allows the mice to maintain a normal body temperature.

Accumulation of amyloid plaques, which might be a result of alterations in APP processing or in Aβ clearance, is considered one of the pathological hallmarks of AD [24]. To examine the effects of chronic RF-EMF in AD, we investigated the Aβ burden in the 5xFAD mice brain. At the age of 9.5 months, an accumulation of Aβ was found in hippocampus and cortex of 5xFAD mice, which was consistent with previous study [19]. However, chronic RF-EMF exposure reduced accumulation of Aβ significantly in the brain tissue of the 5xFAD mice, and reduced Aβ might be mainly Aβ42 than Aβ40, which was examined by ELISA. Because the APP is the precursor of Aβ, APP processing and degrading enzymes were examined in 5xFAD mice. Interestingly, the expressions of APP and CTFs of APP were increased in the brain of 5xFAD mice,

whereas RF-EMF exposure significantly reduced the levels of those proteins. However given the fact that the levels of the Aβ-degrading enzymes were not significantly affected suggested that the effects of RF-EMF on the APP/Aβ42 might be related with the down-regulation of APP, not with the clearance of Aβ. However we don't know how RF-EMF affects on down-regulation of APP in the present study. Because we analyzed brain samples receiving chronic RF-EMF exposure, we could not know whether RF-EMF affects on APP processing or APP producing. Therefore, to identify exact mechanism of RF-EMF on APP processing and APP production, further studies with various periods for RF-EMF exposure will be needed.

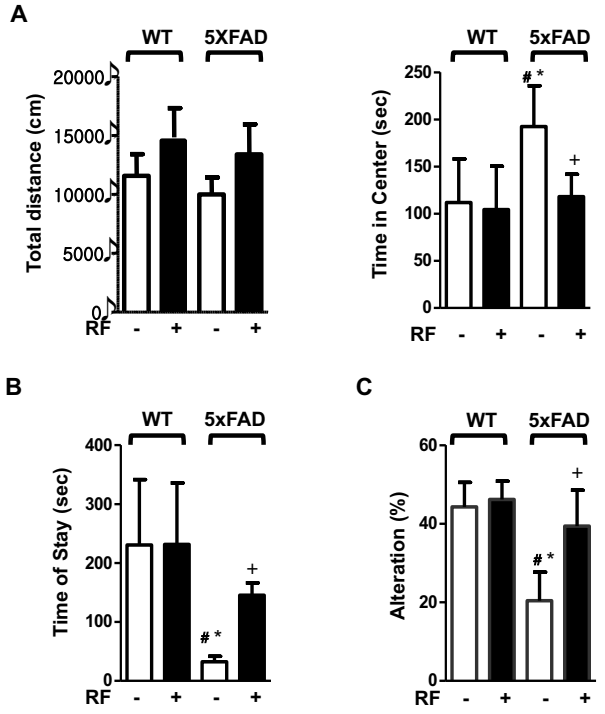

Fig. (5). RF-EMF attenuates memory impairment in Tg-5xFAD mice. A. Open field tests were conducted for general activity/exploratory activity. Total distance traveled and the amount of time the mice stayed in the center zone was measured. **B.** Passive avoidance tests were performed to evaluate memory impairment in Tg-5xFAD and WT mice following RF-EMF exposure. An electric shock was given to the mice when they entered the light room from the dark room on the first day. The amount of time the mice stayed in the light room without shock was also measured. The graph represents the amount of time the mice stayed in the light room. **C.** The Y-maze test was performed to evaluate spatial memory in mice. Alteration indicates percentage of frequency of non-overlapped entry compared to the total number of entries in the 3 arms. Values are presented as the mean ± SEM (n = 7) and analyzed by ANOVA (analysis of variance) and Bonferroni post-hoc test (# $p < 0.05$ *vs*. WT-RF(-), * $p < 0.05$ *vs*. WT-RF (+), + $p < 0.05$ *vs*. Tg-5xFAD-RF (-)).

Our study showed that chronic RF-EMF exposure had beneficial effects in AD mice. The Tg-5xFAD mice showed serious accumulation of Aβ and neuroinflammation, much more impaired memory functions, and late stages of AD-like pathology. RF-EMF not only reduced parenchymal Aβ accumulation but also BACE1 expression, which is a key enzyme that cleaves Aβ from APP in the brain [25, 26], and inhibits the neuroinflammation response in Tg-5xFAD mice (Fig. **4**). Arendash GW reported that RF-EMF directly reduced Aβ deposition by inhibiting Aβ oligomerization and enhancing monomer type to blood vessel excretion (reviewed in [18]). Even though Tg-5xFAD mice could genetically manufacture and produce Aβ42 [23], decreased BACE1 levels which are mediated by RF-EMF exposure could affect Aβ42 production. Increased extracellular accumulation of Aβ, in particular Aβ42, resulted in the formation of Aβ oligomers, cerebral amyloid plaques, neurodegeneration and ultimately, brain atrophy [27]. Also it has been reported that BACE1 has a critical role in Aβ pathology and BACE1 inhibition rescues memory deficits [28-30]. Therefore, our data suggested that RF-EMF has beneficial effects on Aβ pathology of AD via inhibition of accumulated Aβ plaques and BACE1 expression in brain parenchyma (Figs. **1** and **3**), which is the first report that RF-EMF could modulate BACE1 in the brain of mice.

In addition, RF-EMF inhibited activated glial cells known to participate in Aβ clearance by producing a number of Aβ degrading enzymes [31]. RF-EMF dramatically reduced reactive microglia and active astrocytes in the brain section of AD (Fig. **4B**). Microglia, the resident inflammatory cells of the brain, are highly activated in the AD brain [32, 33]. Activated immune response within the brain is a classic feature of neurodegenerative disease such as AD and Parkinson's disease. Despite different triggering events, a common feature is chronic immune activation, in response to microglia, and the resident macrophages of the central nerve system [34]. RF-EMF significantly inhibited reactive microglia in the brain tissue of AD mice.

To further explore the effects of RF-EMF on brain function, we performed very simple behavioral tests of memory function such as passive avoidance test and Y-maze. Despite RF-EMF exposure was more beneficial on Aβ pathology in the hippocampus than the cortex region, we did not perform hippocampus-dependent behavioral tests such as Morris water maze because Tg-5xFAD mice had already exhibited motor impairment at 9.5 months of age, as earlier observed by Jawhar *et al.* [35]. Tg-5xFAD mice at 9.5 months of age were impaired both non-spatial and spatial memory, as evidenced in the passive avoidance and Y-maze tests, compared to WT animals and such memory impairments improved significantly upon exposure to RF-EMF (Fig. **5**), suggesting that RF-EMF protects against brain functional impairment associated with late AD-like pathology.

Our results on the effects of RF-EMF in WT are conflicting with Tg-5xFAD mice even if we used age-matched mice. Chronic RF exposure in our experimental condition did not show any effects on WT including Aβ pathology in tissue and brain function. Contrary to RF-EMF effect on AD mice, chronic RF slightly increased BACE1 and GFAP level in brain tissue (Figs. **3B** and **4B**). However WT did not show any consequential Aβ deposition and memory impairment at 9.5 months of age (Figs. **1B** and **5**). Some papers suggested that RF-EMF had harmful effect [8-11] or no influence [12, 13] in WT. Ammari *et al.* also reported that GFAP

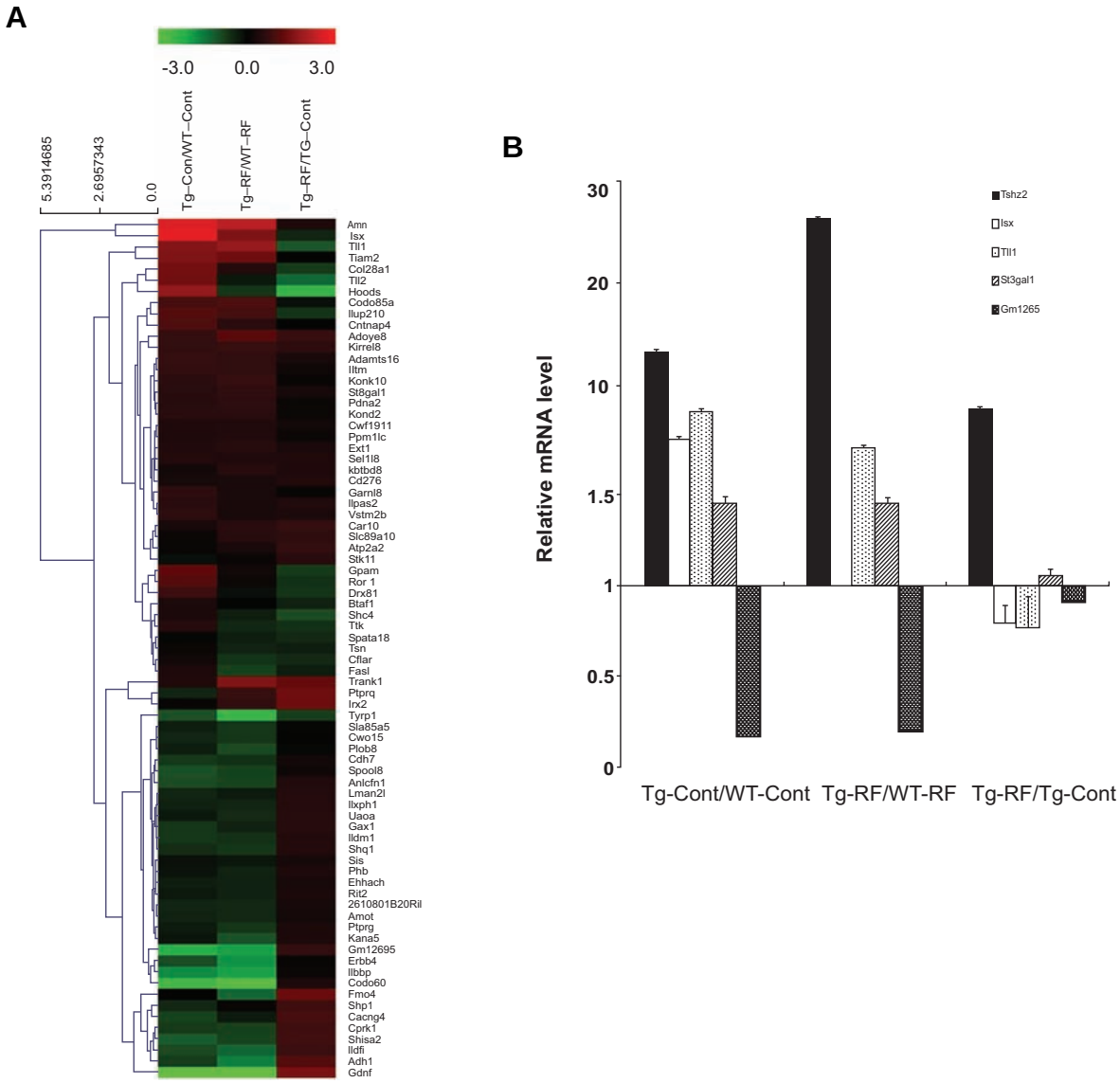

Fig. (6). Altered psychology-related gene expression following RF-EMF. A. A Cluster heat map of genes whose expression was significantly altered in the hippocampus of WT and Tg-5xFAD mice with or without RF-EMF exposure. In the heat map, green represents a lower expression level and red indicates a higher expression level. **B.** A qRT-PCR for 5 genes was performed using 3 different hippocampus samples from WT and Tg-5xFAD mice with or without RF-EMF exposure. Values are presented as the mean ± SEM and analyzed by ANOVA (analysis of variance) and Bonferroni post-hoc test.

Table 4. The list of candidate genes.

		Fold Change		
Gene Symbol	**Description**	**RF WT/Con WT**	**RF TG/Con TG**	**Con TG/Con WT**
Tshz2	Teashirt zinc finger family member 2	7.05	9.86	1.12
Isx	Intestine specific homeobox	6.73	2.91	0.74
Tll1	Musmusculustolloid-like	2.99	3.49	0.5
St3gal1	ST3 beta-galactoside alpha-2,3-sialyltransferase 1	3.07	3.95	1.15
Gm12695	Predicted gene 12695	0.23	0.27	1.63

expression was increased by RF-EMF exposure [36]. The differences in GFAP expression that are induced by RF-EMF exposure between WT and Tg mice could be attributable to the fact that Ammari *et al.* used rats and we used mice. Another difference was the exposure duration. Ammari *et al.* examined GFAP expression after acute RF-EMF exposure (for 3 to 10 days exposure), however, we exposed chronically (8 months). However, even GFAP expression level in the brain after RF-EMF exposure was higher than that of control WT mice, and RF-EMF reduced reactive microglia. There is no report of alterations of BACE1 by RF-EMF. It should seem that WT did not produce enough APP altered by BACE1 or immune cells and there is another mechanism to maintain homeostasis of the brain. However, these data indicated that RF-EMF did not have any effects on the brain of WT mice and also suggested that the possibility of RF-EMF effecting directly on Aβ pathology of AD brain.

We also performed cDNA microarray using the hippocampus from WT and Tg-5xFAD mice following RF-EMF exposure to identify genes responsible for brain functions. We analyzed gene profiles that were categorized according to the brain functions (Supplementary Table **1**) and selected genes which were differentially expressed in AD mice (more than 2-fold up or down). Five genes were selected after confirmation by qRT-PCR using hippocampal tissues. The RF-EMF effect appears to have an opposite expression impact between WT and Tg-5xFAD mice and even the RF-EMF-exposed hippocampus in WT mice showed similar gene expression patterns with that of control Tg-5xFAD without RF-EMF exposure. The Tshz2, Gm12695 and St3gal1 genes were altered in Tg-5xFAD mice when compared to WT mice and RF-EMF exposure to WT or Tg-5xFAD mice also affected expression in similar patterns, suggesting that these genes might be related to AD development and that RF-EMF accelerated these gene alterations. Other genes such as Isx, and Tll1 were shown to have similar expression patterns between RF-EMF-exposed WT and control Tg-5xFAD mice when control WT mice were used as control. However, these expression patterns were reversed in Tg-5xFAD RF-EMF-exposed mice, suggesting the RF-EMF specific genes for beneficial brain functions in AD mice. Further detailed mechanism studies are needed to confirm this hypothesis.

Interestingly, it has been reported that five genes were found to be related to Aβ directly or indirectly. Gene Isx has been reported to interact with HSP90-client (HSP90AA1) [37], and HSP90 was reported to attenuate the accumulation of Aβ42 [38]. The Tshz2 gene has not been reported to be related to AD; however Tshz3, which is an isomer of Tshz2, is known to have reduced expression in AD [39]. It has also been reported that St3gal1 has four N-glycan attachment sites in its catalytic domain that are potentially glycosylated [40]. Moreover, BACE1 is known to have several N-linked glycosylation sites and N-glycosylation is important for enzymatic activity of BACE1 [28]. Gm12695 and Tll1 have been reported to interact with oligomeric Aβ42 in protein array [41]. Although in this study we do not clarify that these genes are involved in the protection or pathogenic mechanism of AD pathology, it is evident that RF-EMF affects gene expression of brain function and therefore, the mechanism of RF-EMF effect on AD should be investigated further.

We do not know how RF-EMF ameliorates Aβ pathology in AD brain. However, we have shown that RF-EMF prevents Aβ deposition in the brain parenchyma and, especially, we show here in (for the first time) that RF-EMF modulates APP and BACE1 levels. Future work should clarify the critical time-points for and targets of RF-EMF exposure, to discover the mechanism whereby RF-EMF inhibits parenchymal Aβ deposition and modulates BACE1 expression.

CONCLUSION

Our results showed that RF-EMF ameliorates AD-like pathology in Tg-5xFAD mice via Aβ modulation. The mechanism underlying the anti-memory impairment action of RF-EMF can directly inhibit Aβ production by suppressing APP and BACE1 expression and indirectly regulate gene expression for Aβ production and reduce neuroinflammation. Our findings suggest that RF-EMF has a potential role in AD pathogenesis.

CONFLICT OF INTEREST

The authors confirm that this article content has no conflict of interest.

ACKNOWLEDGEMENTS

We thank Professor Inhee Mook-Jung for providing the Tg-5xFAD mice.

This work was supported by ICT R&D program of MSIP/IITP. [13-911-01-105, A Study on Health Effects and Protection of EMF] and was also supported by a grant (14172MFDS431) from Ministry of Food and Drug Safety in 2014.

CONTRIBUTION OF AUTHORS

Designed research/study: Hae-June Lee, Yun-Sil Lee, JongHwa Kwon

Contributed important reagent: Hyung-Do Choi, Jeong-Ki Pack, Nam Kim

Performed research/study: Ye Ji Jeong, Ga-Young Kang, Hae-June Lee

Wrote paper: Hae-June Lee, Yun-Sil Lee

The English in this document has been checked by Eureka Science.

SUPPLEMENTARY MATERIAL

Supplementary material is available on the publisher's web site along with the published article.

REFERENCES

[1] Hardell L, Carlberg M, Soderqvist F, Mild KH. Case-control study of the association between malignant brain tumours diagnosed between 2007 and 2009 and mobile and cordless phone use. Int J Oncol 43: 1833-1845 (2013).

[2] Kesari KK, Siddiqui MH, Meena R, Verma HN, Kumar S. Cell phone radiation exposure on brain and associated biological systems. Indian J Exp Biol 51: 187-200 (2013).

[3] Habash RW, Elwood JM, Krewski D, Lotz WG, McNamee JP, Prato FS. Recent advances in research on radiofrequency fields and health: 2004-2007. J Toxicol Environ Health B Crit Rev 12: 250-288 (2009).

[4] INTERPHONE Study Group. Brain tumour risk in relation to mobile telephone use: results of the INTERPHONE international case-control study. Int J Epidemiol 39: 675-694 (2010).

[5] Carlberg M, Soderqvist F, Hansson Mild K, Hardell L. Meningioma patients diagnosed 2007--2009 and the association with use of mobile and cordless phones: a case--control study. Environ Health 12: 60 (2013).

[6] Kan P, Simonsen SE, Lyon JL, Kestle JR. Cellular phone use and brain tumor: a meta-analysis. J Neurooncol 86: 71-78 (2008).

[7] Szmigielski S. Cancer risks related to low-level RF/MW exposures, including cell phones. Electromagn Biol Med 32: 273-280 (2013).

[8] Jiang DP, Li J, Zhang J, Xu SL, Kuang F, Lang HY, *et al.* Electromagnetic pulse exposure induces overexpression of beta amyloid protein in rats. Arch Med Res 44: 178-184 (2013).

[9] Ntzouni MP, Skouroliakou A, Kostomitsopoulos N, Margaritis LH. Transient and cumulative memory impairments induced by GSM 1.8 GHz cell phone signal in a mouse model. Electromagn Biol Med 32: 95-120 (2013).

[10] Aldad TS, Gan G, Gao XB, Taylor HS. Fetal radiofrequency radiation exposure from 800-1900 mhz-rated cellular telephones affects neurodevelopment and behavior in mice. Sci Rep 2: 312 (2012).

[11] Ntzouni MP, Stamatakis A, Stylianopoulou F, Margaritis LH. Short-term memory in mice is affected by mobile phone radiation. Pathophysiology 18: 193-199 (2011).

[12] Maaroufi K, Had-Aissouni L, Melon C, Sakly M, Abdelmelek H, Poucet B, *et al.* Spatial learning, monoamines and oxidative stress in rats exposed to 900 MHz electromagnetic field in combination with iron overload. Behav Brain Res 258: 80-89 (2014).

[13] Sienkiewicz ZJ, Blackwell RP, Haylock RG, Saunders RD, Cobb BL .Low-level exposure to pulsed 900 MHz microwave radiation does not cause deficits in the performance of a spatial learning task in mice. Bioelectromagnetics 21: 151-158 (2000).

[14] Banaceur S, Banasr S, Sakly M, Abdelmelek H. Whole body exposure to 2.4 GHz WIFI signals: effects on cognitive impairment in adult triple transgenic mouse models of Alzheimer's disease (3xTg-AD). Behav Brain Res 240: 197-201 (2013).

[15] Arendash GW, Mori T, Dorsey M, Gonzalez R, Tajiri N, Borlongan C. Electromagnetic treatment to old Alzheimer's mice reverses beta-amyloid deposition, modifies cerebral blood flow, and provides selected cognitive benefit. PLoS One 7: e35751 (2012).

[16] Dragicevic N, Bradshaw PC, Mamcarz M, Lin X, Wang L, Cao C, *et al.* Long-term electromagnetic field treatment enhances brain mitochondrial function of both Alzheimer's transgenic mice and normal mice: a mechanism for electromagnetic field-induced cognitive benefit? Neuroscience 185: 135-149 (2011).

[17] Arendash GW, Sanchez-Ramos J, Mori T, Mamcarz M, Lin X, Runfeldt M, *et al.* Electromagnetic field treatment protects against and reverses cognitive impairment in Alzheimer's disease mice. J Alzheimers Dis 19: 191-210 (2010).

[18] Arendash GW. Transcranial electromagnetic treatment against Alzheimer's disease: why it has the potential to trump Alzheimer's disease drug development. J Alzheimers Dis 32: 243-266 (2012).

[19] Oakley H, Cole SL, Logan S, Maus E, Shao P, Craft J, *et al.* Intraneuronal beta-amyloid aggregates, neurodegeneration, and neuron loss in transgenic mice with five familial Alzheimer's disease mutations: potential factors in amyloid plaque formation. J Neurosci 26: 10129-10140 (2006).

[20] Moon M, Cha MY, Mook-Jung I. Impaired Hippocampal Neurogenesis and its Enhancement with Ghrelin in 5XFAD Mice. J Alzheimers Dis 41: 233-241 (2014).

[21] Lee HJ, Jin YB, Kim TH, Pack JK, Kim N, Choi HD, *et al.* The effects of simultaneous combined exposure to CDMA and WCDMA electromagnetic fields on rat testicular function. Bioelectromagnetics 33: 356-364 (2011).

[22] Paxinos G, Franklin K. In:Paxinos and Franklin's the Mouse Brain in Stereotaxic Coordinates.Elsevier Science & Technology Book fourth edition (2012).

[23] Eimer WA, Vassar R. Neuron loss in the 5XFAD mouse model of Alzheimer's disease correlates with intraneuronal Abeta42 accumulation and Caspase-3 activation. Mol Neurodegener 8: 2 (2013).

[24] Selkoe DJ. Amyloid beta protein precursor and the pathogenesis of Alzheimer's disease. Cell 58: 611-612 (1989).

[25] Jeppsson F, Eketjall S, Janson J, Karlstrom S, Gustavsson S, Olsson LL, *et al.* Discovery of AZD3839, a potent and selective BACE1 inhibitor clinical candidate for the treatment of Alzheimer disease. J Biol Chem 287: 41245-41257 (2012).

[26] Xu Y, Li MJ, Greenblatt H, Chen W, Paz A, Dym O, *et al.* Flexibility of the flap in the active site of BACE1 as revealed by crystal structures and molecular dynamics simulations. Acta Crystallogr D Biol Crystallogr 68: 13-25 (2012).

[27] Hardy J, Selkoe DJ. The amyloid hypothesis of Alzheimer's disease: progress and problems on the road to therapeutics. Science 297: 353-356 (2002).

[28] Cole SL, Vassar R. The Alzheimer's disease beta-secretase enzyme, BACE1.Mol Neurodegener 2: 22 (2007).

[29] Menting KW, Claassen JA. β-secretase inhibitor; a promising novel therapeutic drug in Alzheimer's disease. Front Aging Neurosci 6:165 (2014).

[30] Yan R, Vassar R. Targeting the β secretase BACE1 for Alzheimer's disease therapy. Lancet Neurol 13(3): 319-29 (2014).

[31] Von Bernhardi R. Glial cell dysregulation: a new perspective on Alzheimer disease. Neurotox Res 12: 215-232 (2007).

[32] Akiyama H, Barger S, Barnum S, Bradt B, Bauer J, Cole GM, *et al.* Inflammation and Alzheimer's disease. Neurobiol Aging 21: 383-421(2000).

[33] Wyss-Coray T, Mucke L. Inflammation in neurodegenerative disease--a double-edged sword. Neuron 35: 419-432 (2002).

[34] Amor S, Puentes F, Baker D, van der Valk P. Inflammation in neurodegenerative diseases. Immunology 129: 154-169 (2010).

[35] Jawhar S, Trawicka A, Jeenneckens C, Bryer TA, Wirths O. Motor deficits, neuron loss, and reduced anxiety coinciding with axonal degeneration and intraneuronal Aβ aggregation in the 5XFAD mouse model of Alzheimer's disease. Neurobiol Aging 33(1):196e29-40 (2012).

[36] Ammari M, Gamez C, Lecomte A, Sakly M, Abdelmelek H, De Seze R. GFAP expression in the rat brain following sub-chronic exposure to a 900 MHz electromagnetic field signal. Int J Radiat Biol 86: 367-375 (2010).

[37] Taipale M, Krykbaeva I, Koeva M, Kayatekin C, Westover KD, Karras GI, *et al.* Quantitative analysis of HSP90-client interactions reveals principles of substrate recognition. Cell 150: 987-1001(2012).

[38] Kumar P, Ambasta RK, Veereshwarayya V, Rosen KM, Kosik KS, Band H, *et al.* CHIP and HSPs interact with beta-APP in a proteasome-dependent manner and influence Abeta metabolism. Hum Mol Genet 16: 848-864 (2007).

[39] Kajiwara Y, Akram A, Katsel P, Haroutunian V, Schmeidler J, Beecham G, *et al.* FE65 binds Teashirt, inhibiting expression of the primate-specific caspase-4. PLoS One 4: e5071 (2009).

[40] Jeanneau C, Chazalet V, Auge C, Soumpasis DM, Harduin-Lepers A, Delannoy P, *et al.* Structure-function analysis of the human sialyltransferase ST3Gal I: role of n-glycosylation and a novel conserved sialylmotif. J Biol Chem 279: 13461-13468 (2004).

[41] Olah J, Vincze O, Virok D, Simon D, Bozso Z, Tokesl N, *et al.* Interactions of pathological hallmark proteins: tubulin polymerization promoting protein/p25, beta-amyloid, and alpha-synuclein. J Biol Chem 286: 34088-34100 (2011).

Received: December 17, 2014 **Revised: March 16, 2015** **Accepted: March 21, 2015**